Supporting Information

MnS/MnO-coated N, S-doped Carbon Anode obtained from a Mn(II)-coordinated Polymer for Long-cycle Life Li-ion Batteries

Kyubin Shim[a1], Hyun Woo Kim[a1], Sungwoo Park[a], Kyeong-Deok Seo[b], Chang-Yeon Kim[a], Jin Bae Lee[a], Jong Seong Bae[c] and Hae Jin Kim[a]*

[a] Research Center for Materials Analysis, Korea Basic Science Institute, Daejeon 34133, Republic of Korea

[b] Department of Chemistry and Chemistry Institute for Functional Materials, Pusan National University, Busan 46241, Republic of Korea

[c] Busan Center, Korea Basic Science Institute, Busan 46742, Republic of Korea

[*] Corresponding author: H. J. Kim; E-mail address: hansol@kbsi.re.kr

[1]The first two authors contributed equally to this work.

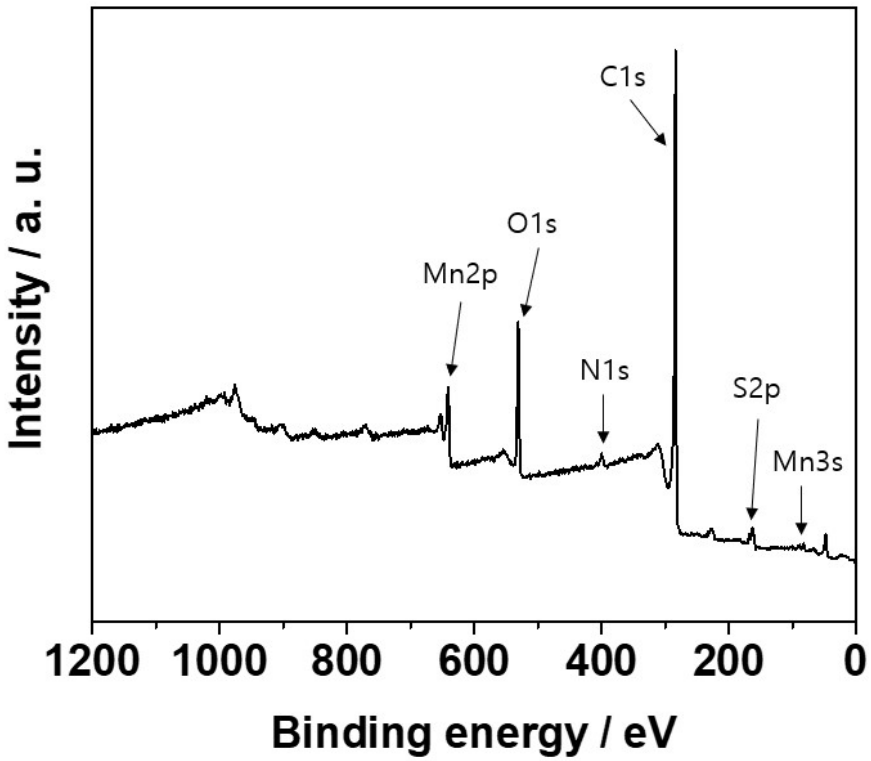

Figure S1. XPS survey spectra of MSNC (powder samples).

Table S1. Peak positions of the XPS (powder sample)

(Unit: eV)

C1s			N1s			O1s		
C-C	C-O/C-N/C-S	C=O	Pyrrolic-N	quaternary-N	Pyndinic-N	Metal-O	C-O	C=O
284.61	285.77	288.36	400.59	401.66	398.46	529.62	531.39	533.05
S2p			**Mn2p**					
C-S-C	MnS	Sulphate	Mn^{2+} (MnO)	Mn^{2+} (MnS)	$Mn^{3+,4+}$	Mn^{2+} satellite		
163.57/164.78	160.81/162.08	168.23	640.77	642.41	644.08	646.77		

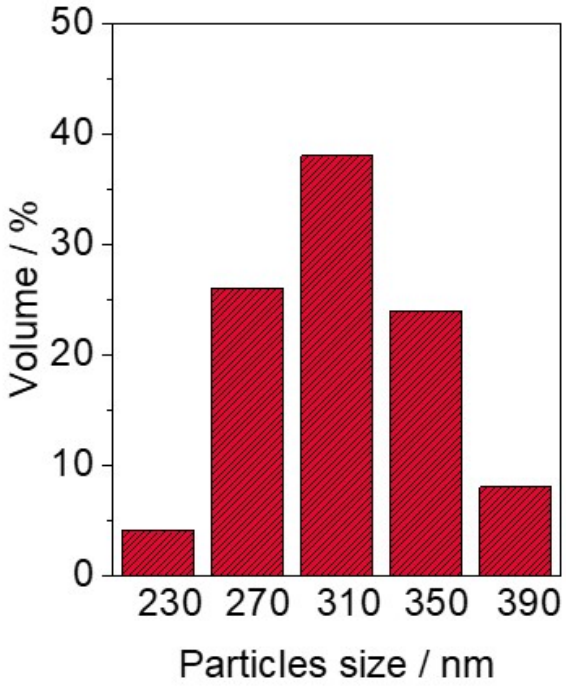

Figure S2. Size distribution of MSMC powders.

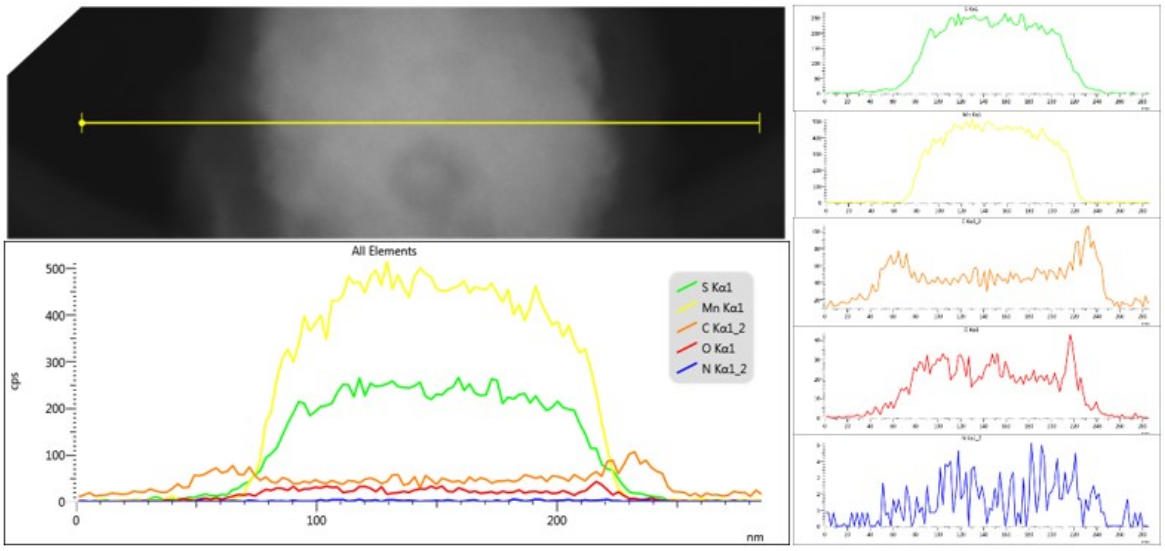

Figure S3. Line profile of the core-shell structure for MSNC.

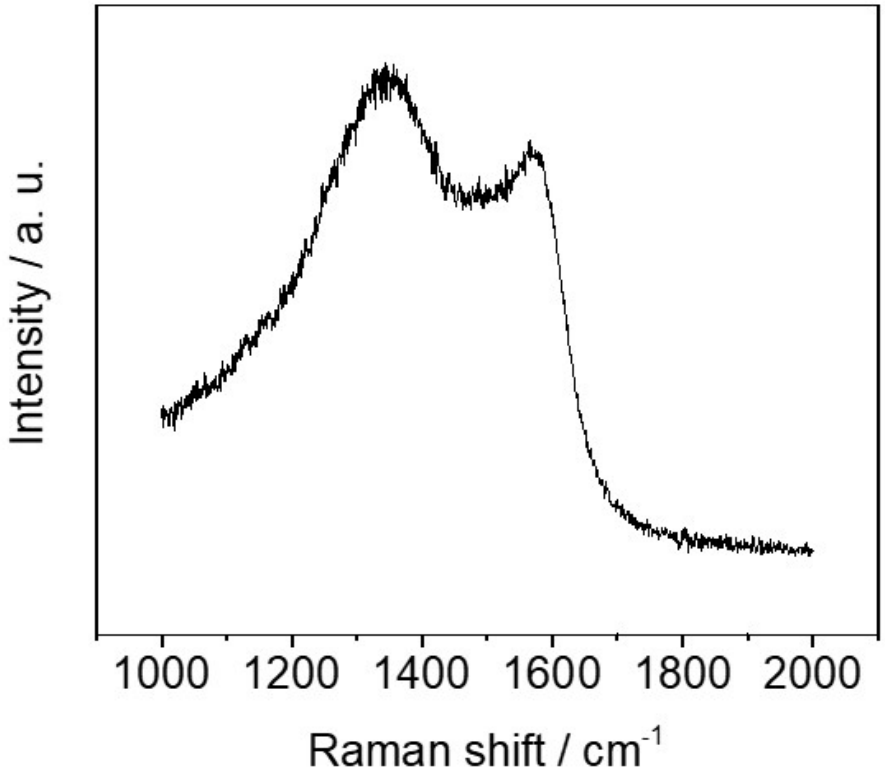

Figure S4. Electrochemical active surface area (ECSA) test using the double-layer capacitance of the MSNC.

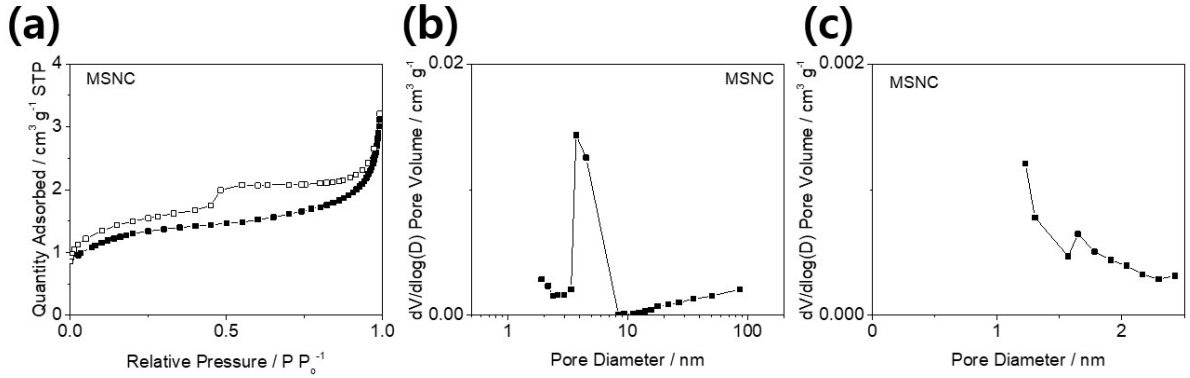

Figure S5. (a) N_2 adsorption-desorption isotherms of the sample at 77K. (b) Pore size distributions of the samples obtained by the BJH method (desorption branch) and (c) the HK method (adsorption branch).

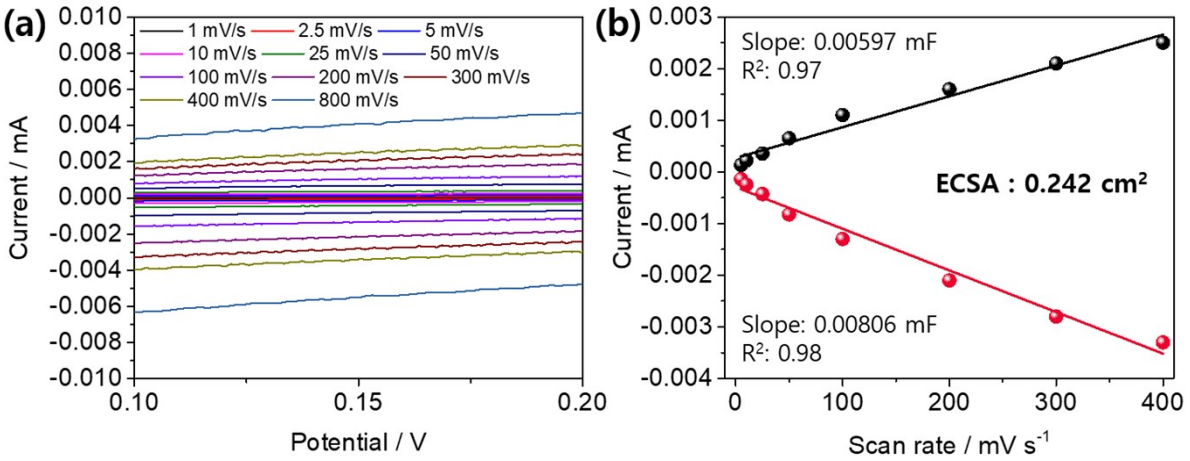

Figure S6. Electrochemical active surface area (ECSA) test using the double-layer capacitance of the MSNC.

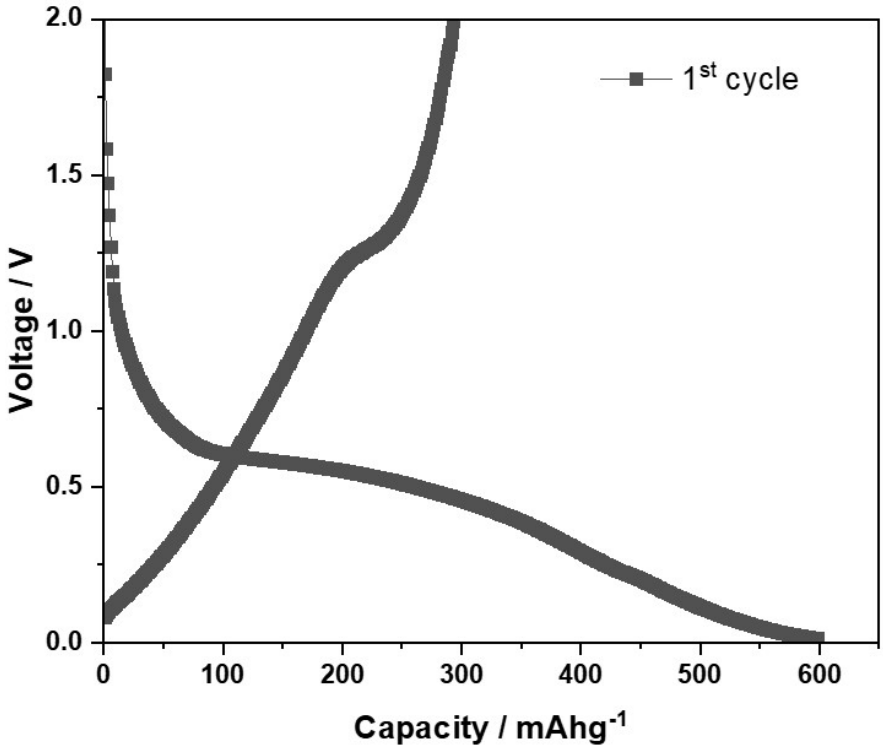

Figure S7. Discharge/charge profile of the Li/MSNC cell for the 1st cycle.

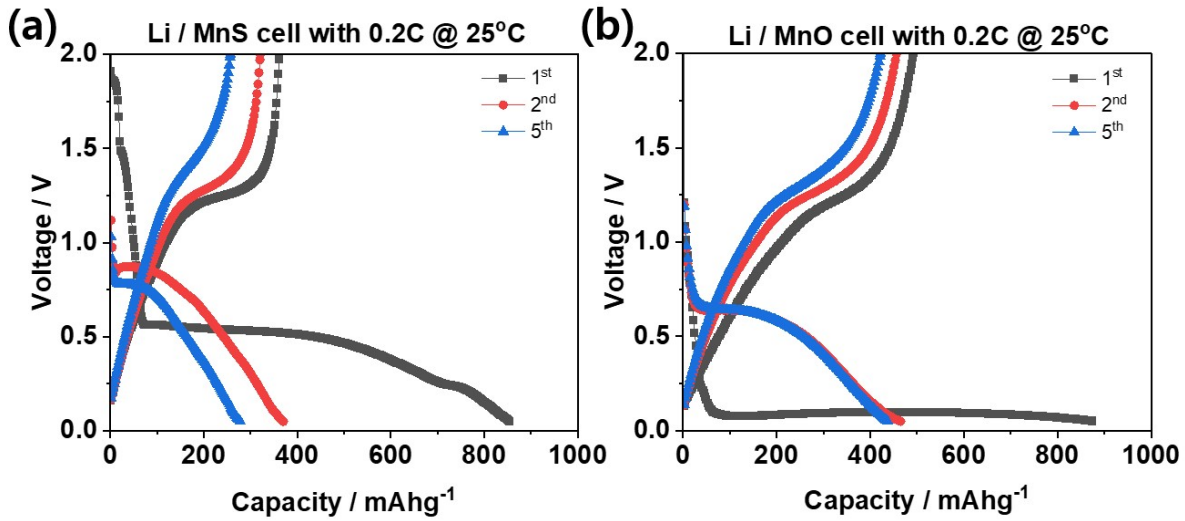

Figure S8. Discharge/charge profile of the for the 1st , 2 nd, and 5 th cycle (a) Li/MnS cell, (b) Li/MnO cell

Figures S8 illustrates the discharge/charge curves of the MnS and MnO electrode for 5 cycles at a rate of 0.2C, ranging from 0.05 to 2.0 V. The MnS and Mno electrode initially exhibits discharge and charge capacities of 854 and 357 mA h g^{-1}(MnS), 880 and 495 mA h g^{-1} (MnO), respectively.

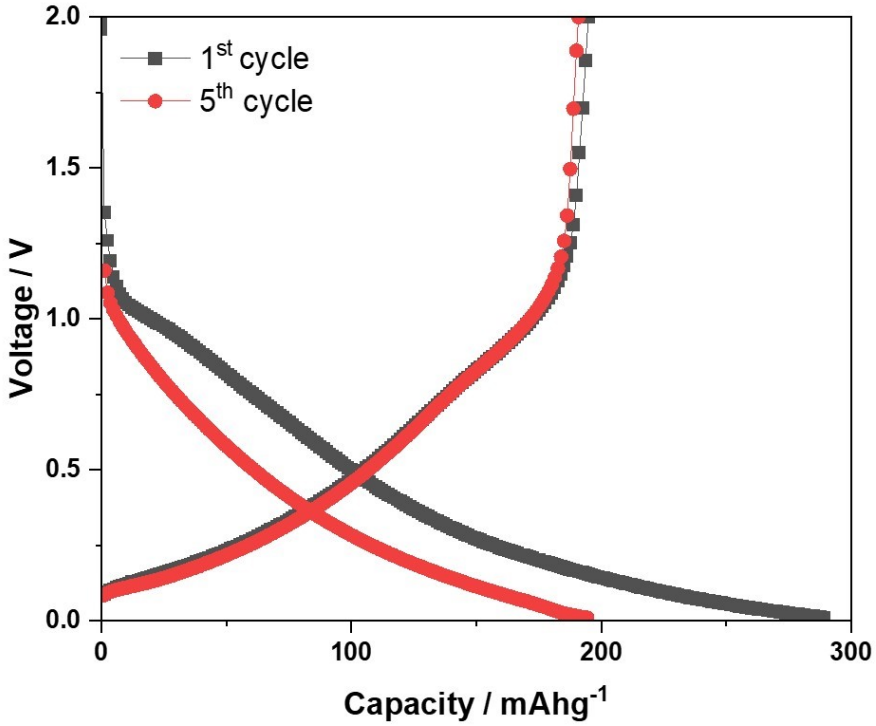

Figure S9. Discharge/Charge profile of the Li/HC cell.

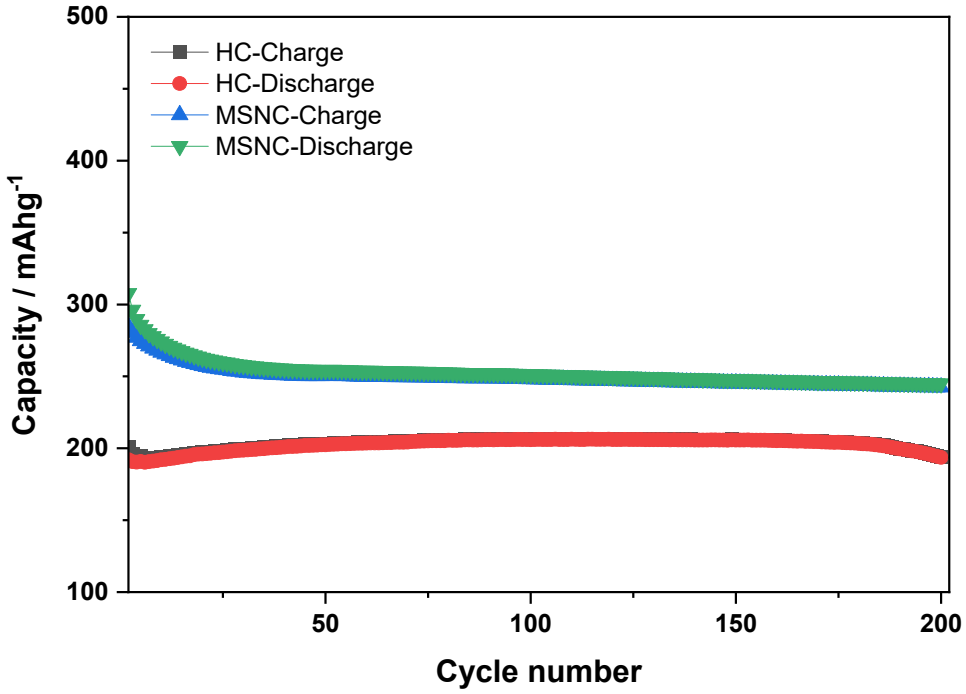

Figure S10. Comparison of the cyclability of MSNC and HC cells for up to 200 cycles with 0.2 C.

Table S2. Electrochemical performances comparison of MSNC anodes with recently reported Mn-based carbon composite anodes

	Composition	Organic compounds (%)	Initial electrochemical performances				Cycle stability (mAh/g @ n cycle)
			Discharge (mAh/g)	Charge (mAh/g)	Current density (mA/g)	Voltage cut-off (V)	
This work	MnS/MnO@ N,S-C	71.34	598	293	74.4	0.05 - 2	232 @ 500
R1	MnO/MnS@ N,S-C	20.45	535	530	100	0.01 - 3	574 @ 500
R2	2AQ-MnO_2	73.3	965.7	465.6	100	0.005 - 3	756 @ 200
R3	MnO/MnS-C	-	~1480	~980	100	0.01 - 3	534 @ 300
R4	MnO/C	46.3	~2130	~ 1100	100	0.05 - 3	741 @ 300
R5	MnO@C/C NTs	19.41	1089	735	200	0.05 - 3	1266 @ 300
R6	α-MnS/C	35.9	~900	~ 590	200	0.01 - 3	672 @ 200
R7	MnS@N,S-C	-	840	750	100	0.01 - 3	282 @ 500

[R1] K. Wang, K. Zhao, Y. Wang, H. Li, H. Jiang, L. Chen, N, S co-doped carbon confined MnO/MnS heterostructures derived from a one-step pyrolysis of Mn-methionine frameworks for advanced lithium storage, J. Alloys compd., 2021, **860**, 158451.

[R2] Y. Cao, W. Sun, C. Guo, L. Zheng, M. Yao, Y. Wang, Rational Construction of Yolk-Shell Bimetal Modified Quinonyl-Rich Covalent Organic Polymers with Ultralong Lithium-Storage Mechanism, ACS Nano, 2022, **16**, 9830-9842.

[R3] S. Ru, H. Xiao, G. Ma, J. Tan, X. Wang, Z. Ai, Facile synthesis of carbon embedded dual phase MnO/MnS nanoparticles composite for superior lithium storage performance, Mater. Lett., 2020, **276**, 128244.

[R4] J. Zhu, X. Zuo, X. Chen, Y. Ding, MOF-derived MnO/C composites as high-performance lithium-ion battery anodes, Synth. Met., 2021, **280**, 116872.

[R5] X. Jiang, W. Yu, H. Wang, H. Xu, X. Liu, Y. Ding, Enhancing the performance of MnO by double carbon modification for advanced lithium-ion battery anodes, J. Mater. Chem. A, 2016, **4**, 920.

[R6] S.Y. Zhu, Y.F. Yuan, P.F. Du, M. Zhu, Y.B. Chen, S.Y. Guo, α-MnS nanoparticles in-situ anchored in 3D macroporous honeycomb carbon as high-performance anode for Li-ion batteries, Appl. Surf. Sci., 2023, **616**, 156619.

[R7] J. Chen, J. Cong, Y. Chen, Q. Wang, M. Shi, X. Liu, H. Yang, MnS nanoparticles embedded in N, S co-doped carbon nanosheets for superior lithium-ion storage, Appl. Surf. Sci., 2020, **508**, 145239.

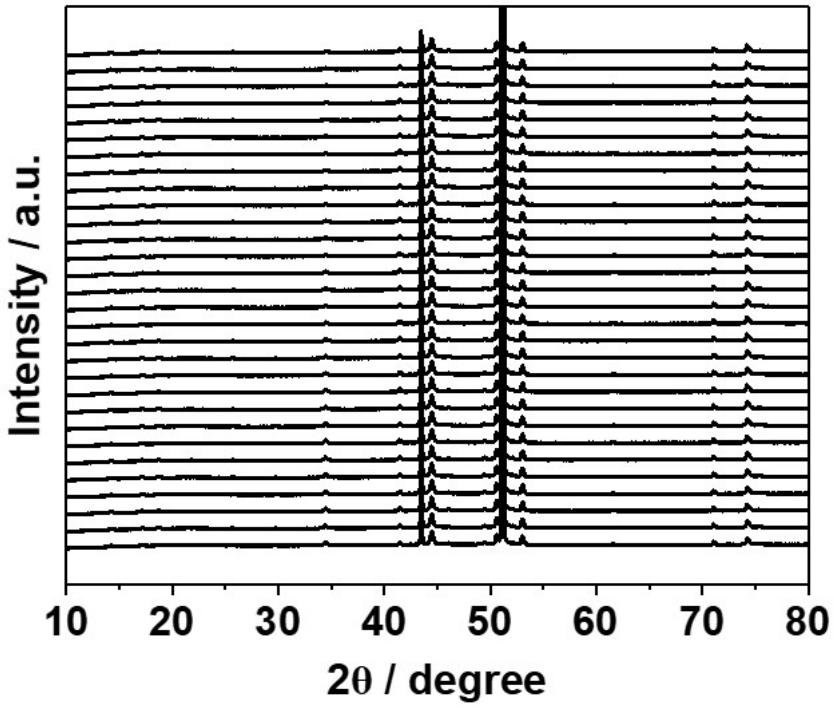

Figure S11. *In-situ* XRD measurements of Li/MSNC cells during discharge/charge.

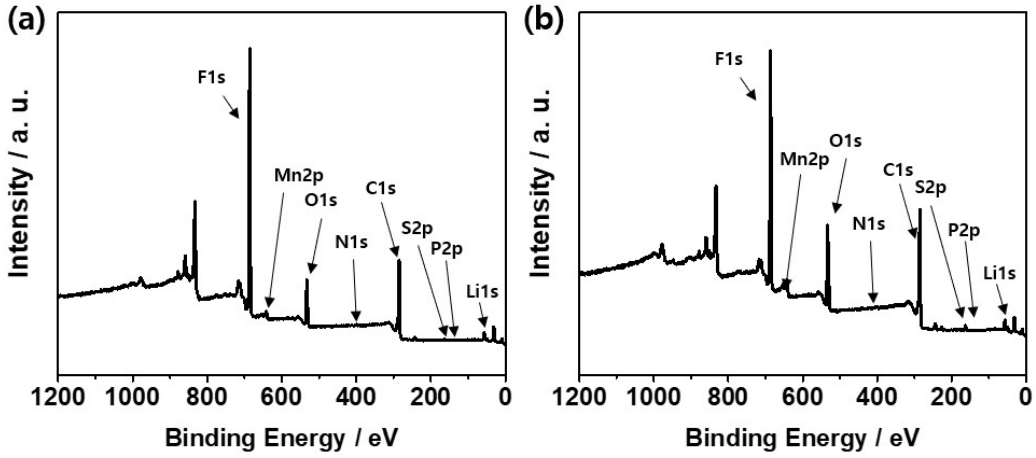

Figure S12. XPS spectra (survey) of the MSNC electrode (a) after one cycle and (b) after 20 cycles.

Table S3. XPS peak positions (after one cycle)

(Unit: eV)

C1s				Mn2P			
C-C	C-O/C-N/C-S	C=O	C-F	Mn^{2+} (MnO)	Mn^{2+} (MnS)	$Mn^{3+,4+}$	Mn^{2+} satellite
284.64	285.85	287.68	289.88	640.30	641.78	644.35	646.98

S2p			O1s			Li1s	
MnS	C-S-C	Sulphate	Li_2O	MnO	C=O	LiF	Li_2O
161.60	162.98	169.74	528.39	529.38	532.20	56.03	56.51

Table S4. XPS peak positions (after 20 cycles)

(Unit: eV)

C1s				Mn2P			
C-C	C-O/C-N/C-S	C=O	C-F	Mn^{2+} (MnO)	Mn^{2+} (MnS)	$Mn^{3+,4+}$	Mn^{2+} satellite
284.60	285.78	287.65	290.75	640.22	641.68	644.29	646.72

S2p			O1s			Li1s	
MnS	C-S-C	Sulphate	Li_2O	MnO	C=O	LiF	Li_2O
161.89	163.21	169.81	529.77	529.59	532.58	56.24	57.24

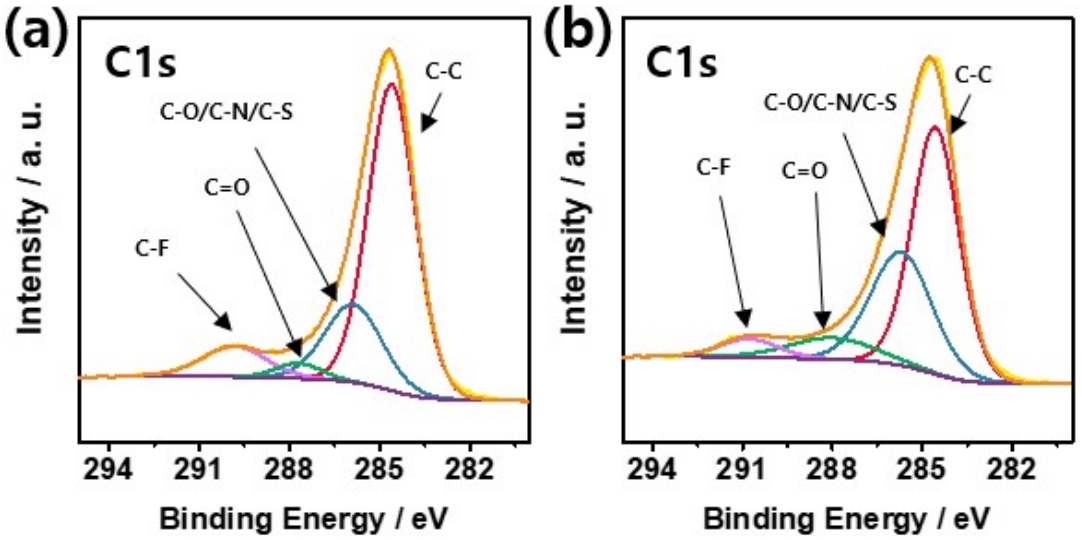

Figure S13. High-resolution C1s spectra of the MSNC electrode (a) after one cycle and (b) after 20 cycles.

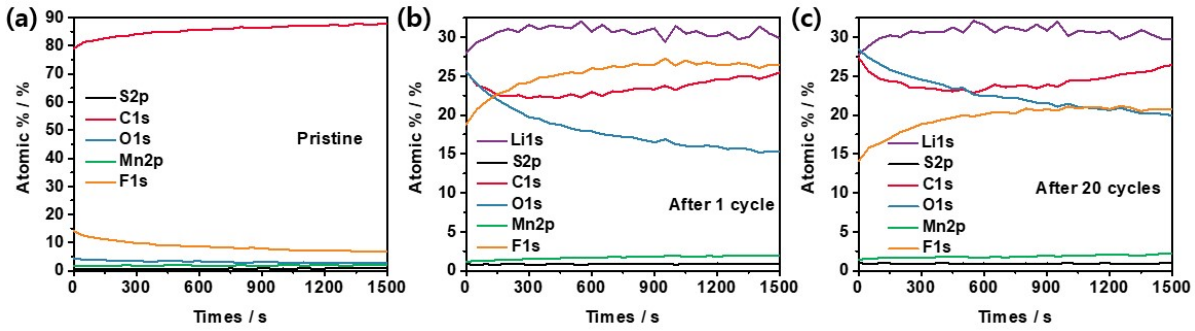

Figure S14. XPS depth study of the MSNC electrode (a) pristine, (b) after one cycle, and (c) after 20 cycles.